

# Joint Planning of Electricity Transmission and Hydrogen Transportation Networks

Siyuan Wang, Rui Bo, *Senior Member, IEEE*

**Abstract**—The abundance and uneven distribution of renewable energy might cause congestion and curtailment in electric power systems. Transmission expansions can potentially alleviate transmission congestion and reduce renewable energy curtailment. On the other hand, with the substantial cost reduction of electrolyzer technology and the continuing rise of hydrogen demand, converting surplus renewable energy to hydrogen provides synergistic benefits to power and hydrogen systems, but consequently requires joint planning of the two systems. To this end, we propose a joint planning approach for power transmission and hydrogen transportation networks to coordinately optimize the investment and operation of power and hydrogen infrastructure. In our proposed model, detailed truck routing, pipeline, and hydrogen storage are formulated to quantify the flexibility of hydrogen transportation system. A robust joint planning approach is also proposed to address various uncertainties from renewable energy, electric load, and hydrogen demand. Our numerical simulations show that the proposed joint planning model can save the total system cost, reduce renewable energy curtailment, and increase the utilization level of transmission lines.

**Index Terms**—transmission expansion planning, hydrogen transportation, hydrogen storage, renewable energy.

## NOMENCLATURE

### Indices and Sets

$s, t, d$	Index for scenarios, hourly time periods, daily time periods.
$i, k, z, b$	Index for units, technologies, zones, power system buses.
$m, n$	Index for terminal zones/buses of truck routines, pipelines, or transmission lines.
$\mathcal{TH}_s, \mathcal{TD}_s$	Set of hourly and daily time periods in weekly scenario $s$ .
$\mathcal{S}$	Set of representative weekly scenarios for each season.
$\mathcal{Z}, \mathcal{B}$	Set of zones and buses.
$\mathcal{K}^{\text{tru}}$	Set of candidate truck transportation technologies.
$\mathcal{R}, \mathcal{P}, \mathcal{L}^c, \mathcal{L}$	Set of truck routines, pipelines, existing and candidate transmission lines.

$\mathcal{E}$	Set of candidate centralized hydrogen storage.
$\mathcal{G}, \mathcal{W}, \mathcal{D}$	Set of existing conventional power generators, renewable energy stations, and electric loads.
$\mathcal{HR}, \mathcal{HE}$	Set of candidate methane reformers and electrolyzer.
<b>Parameters</b>	
$T_{k,m,n}$	Number of daily time periods needed for transportation from zone $m$ to zone $n$ with truck technology $k$ .
$NT^{\text{day}}$	Number of hourly time periods in a day.
$n_s$	Number of occurrences for representative weekly scenario $s$ in a year.
$\phi_i$	Efficiency of power-to-hydrogen conversion for electrolyzer $i$ .
$\underline{\gamma}_i, \bar{\gamma}_i, \gamma_i^0$	Normalized lower, upper, and initial bound coefficients for centralized hydrogen storage $i$ .
$\bar{P}_i^{\text{pip}}$	Flow rate limit of pipeline $i$ .
$\bar{E}_i^{\text{pip}}$	Maximum linepack of pipeline $i$ .
$D_{z,s,t}^{\text{hyd}}$	Hydrogen load in zone $z$ and time period $t$ of scenario $s$ .
$F_i$	Capacity of transmission line $i$ .
$x_i$	Reactance of transmission line $i$ .
$\bar{P}_i, \underline{P}_i$	Upper and lower power bound for unit $i$ .
$RU_i, RD_i$	Upward and downward ramp rate for unit $i$ .
$D_{i,s,t}^{\text{ele}}$	Electric load $i$ in time period $t$ of scenario $s$ .
$W_{i,s,t}$	Maximum available power from renewable station $i$ in time period $t$ of scenario $s$ .
$M$	Big-M coefficient.
$IC$	Annualized investment cost of pipelines or transmission lines.
$ICQ$	Annualized truck investment cost per unit capacity for different technologies.
$ICE$	Annualized investment cost per unit energy capacity (in terms of hydrogen quantity) of hydrogen storage.
$ICH$	Annualized investment cost per unit capacity of hydrogen compression or liquefaction systems for truck, pipeline, and storage. Also used for annualized investment cost per unit capacity of hydrogen production for methane reformers.
$OC$	Operation cost for truck transportation, hydrogen production, hydrogen storage, and electric power generation.

### Decision Variables

$\bar{Q}_k$	Total hydrogen quantity capacity for truck transportation technology $k$ .
-------------	--

Manuscript received March 17, 2021; revised June 14, 2021 and August 19, 2021; accepted September 18, 2021. This material is based upon work supported by the U.S. Department of Energy's Office of Energy Efficiency and Renewable Energy (EERE) under the Water Power Technologies Office Award Number DE-EE0008781. The views expressed herein do not necessarily represent the views of the U.S. Department of Energy and the United States Government. Paper no. 2021-ATAH-0159.R2. (*Corresponding author: Rui Bo.*)

The authors are with the Department of Electrical and Computer Engineering, Missouri University of Science and Technology, MO 65409 USA (e-mail: siyuanwang@mst.edu; rbo@mst.edu).

$\overline{H}_{k,z}^{\text{tru}}$	Compression or liquefaction capacities for truck transportation technology $k$ at zone $z$ .
$q_{k,m,n,s,d}^{\text{tru}}$ , $q_{k,m,n,s,d}^{\text{emptru}}$	Hydrogen truck transportation quantity and empty truck capacity that leaves from zone $m$ to zone $n$ at the beginning of day $d$ of scenario $s$ with technology $k$ .
$e_{k,z,s,d}^{\text{tru}}$ , $e_{k,z,s,d}^{\text{emptru}}$	Hydrogen quantity in charged trucks and capacity of empty trucks with technology $k$ that stay in zone $z$ in day $d$ of scenario $s$ .
$h_{k,z,s,d}^{\text{tru ch}}$ , $h_{k,z,s,d}^{\text{tru dc}}$	Hydrogen quantity that charges to and discharges from trucks with technology $k$ in zone $z$ in day $d$ of scenario $s$ .
$w_i$	Binary investment decision for pipeline $i$ .
$\overline{H}_z^{\text{pip}}$	Compression capacity for pipeline injection at zone $z$ .
$q_{z,s,d}^{\text{pip ch}}$ , $q_{z,s,d}^{\text{pip dc}}$	Hydrogen quantity that charges to and discharge from the pipeline network in zone $z$ in day $d$ of scenario $s$ .
$q_{i,s,d}^{\text{pip in}}$ , $q_{i,s,d}^{\text{pip out}}$	Hydrogen net inflow to pipeline $i$ through zonal node $m$ , and net outflow from pipeline $i$ through zonal node $n$ in day $d$ of scenario $s$ , assuming pipeline $i = (m, n)$ .
$e_{i,s,d}^{\text{pip}}$	Linepack of pipeline $i$ in day $d$ of scenario $s$ .
$\overline{E}_i^{\text{sto}}$	Storage capacity in terms of hydrogen quantity for candidate centralized hydrogen storage $i$ .
$\overline{H}_i^{\text{sto}}$	Compression capacity for candidate centralized hydrogen storage $i$ .
$h_{i,s,d}^{\text{sto ch}}$ , $h_{i,s,d}^{\text{sto dc}}$	Hydrogen quantity that charges to and discharges from centralized storage $i$ in day $d$ of scenario $s$ .
$de_{i,s,d}^{\text{sto}}$	Deviation of state of charge (SOC) for centralized storage $i$ in day $d$ of scenario $s$ from initial SOC in this scenario.
$ee_{i,s}^{\text{sto}}$	End SOC for centralized storage $i$ in the last occurrence of scenario $s$ assuming the charge and discharge pattern in scenario $s$ would sequentially repeat $n_s$ times.
$\overline{H}_i$	Capacity for hydrogen production unit $i$ .
$h_{i,s,d}$	Hydrogen quantity from production unit $i$ in day $d$ of scenario $s$ .
$z_i$	Binary investment decision for transmission line $i$ .
$f_{i,s,t}$	Power flow of transmission line $i$ in time period $t$ of scenario $s$ .
$\theta_{b,s,t}$	Phase angle of bus $b$ in time period $t$ of scenario $s$ .
$p_{i,s,t}$	Power generation from unit $i$ or power consumption of electrolyzer $i$ in time period $t$ of scenario $s$ .
$wc_{i,s,t}$	Curtailement of renewable power at station $i$ in time period $t$ of scenario $s$ .

## I. INTRODUCTION

**C**ARBON neutrality targets have been pledged by numerous countries in the world [1]. Renewable electricity would enable a low or zero carbon footprint in hydrogen

production sections as power-to-hydrogen technologies become mature and affordable. On the other hand, the flexibility of hydrogen production and transportation systems can be leveraged to relieve power transmission congestion brought by renewable energy fluctuations. Given the expectation of increasing coupling between electric power systems and hydrogen supply chains in the future, joint planning studies are urgently needed to better coordinate the aforementioned resource complementation.

The plannings of hydrogen transportation and power transmission networks have been widely investigated in the literature in a separate manner:

- On the power system side, transmission expansion planning problems have been studied over a long time on criteria design [2] and optimization model development [3]. In [4], the role of demand response resources in reducing transmission expansions is analyzed for import lines of locational deliverability areas. With increasing needs for renewable energy in power systems, a transmission system planning approach is proposed in [5] for large-scale wind farms. From a bulk power system perspective, bus injection uncertainties from renewable energy sources are further considered in [6], [7].
- On the hydrogen system side, an early work in [8] focuses on the planning of hydrogen filling stations with onsite renewable energy sources and electrolyzers, by assuming limited transportation capabilities in the early stage of hydrogen utilization. With expected cost reductions on both trucks and pipelines in the future, studies on hydrogen transportation network planning have drawn more attention. A transportation model based hydrogen supply system planning approach is proposed in [9], wherein truck is considered for hydrogen transportation. Authors of [10] propose a design and dimensioning method for hydrogen transmission pipeline networks, in which a local search method is used to solve their proposed model.

These works focus on either hydrogen transportation network or power transmission network planning, however haven't investigated the coupling between them.

In planning problems, considering the interactions between power systems and other infrastructures, such as heat [11] and natural gas [12] networks, starts to arouse the interest of researchers. Some recent works also consider the coupling between power systems and hydrogen supply chains. A deterministic optimal investment method is proposed for hydrogen supply chains considering power systems in [13]. In [14], a novel hydrogen supply chain planning approach with flexible hydrogen transmission and storage schedule is proposed, in which the impact of power system is reflected by electricity prices. These pioneering works provide important insights into power-hydrogen interactions, however, the hydrogen transportation and power transmission networks are not jointly planned. A potential disadvantage could be neglecting the flexibility of hydrogen transportation networks in power system transmission expansion planning. To address this need, we propose a joint planning approach for power transmission and hydrogen transportation networks. Our proposed model is

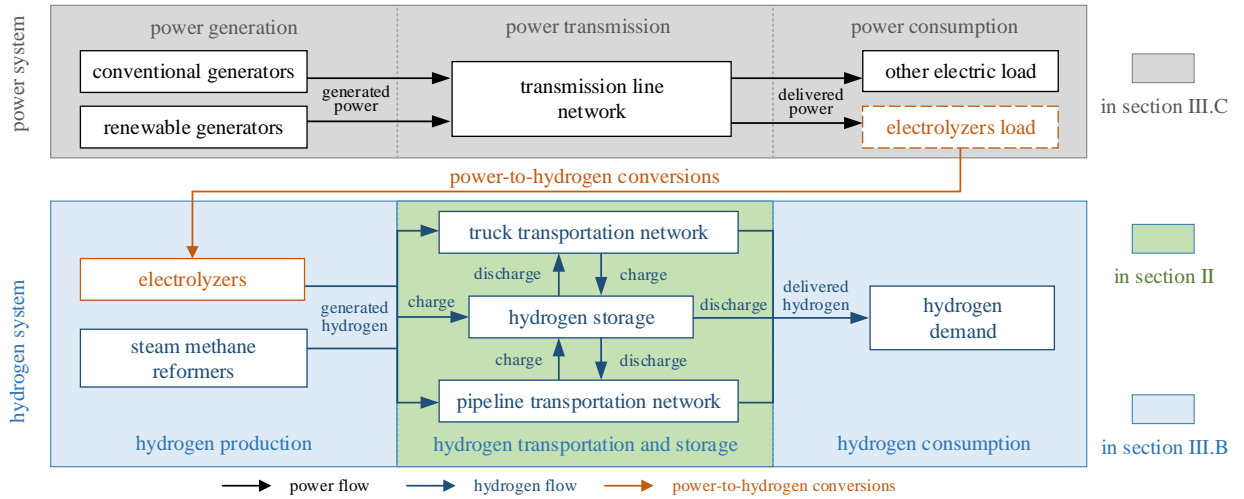


Fig. 1. Framework of integrated power and hydrogen system.

organized under the framework shown in Fig. 1. Furthermore, a robust optimization based joint planning model is developed in this work to address uncertainties from renewable energy, electric load, and hydrogen demand. This model is solved by a column-and-constraint generation (C&CG) algorithm [15]. The proposed approach can offer more reliable investment decisions for transmission expansions and hydrogen supply chains to hedge against the aforementioned uncertainties. It should be noted the same operator of power and hydrogen systems are assumed, as the resource complementation in two physical systems is the main research focus of this work. Future research can continue investigating coordination strategies for different operators.

The modeling of hydrogen transportation network and hydrogen storage in planning problems is an important topic to discuss. (1) For road transportation, hydrogen is transformed into compressed gaseous, liquid, or hydride compound forms. In the literature, the truck transportation system is conventionally modeled based on the classical transport model [9], [13], which is mathematically compact and thus potentially computationally efficient, however, did not properly model the flexibility of truck tanks as storage. This drawback is addressed in [14] through truck-level modeling, which can accurately quantify the flexibility of the truck transportation system. The original integer-based modeling in [14] is computationally expensive, thus a relaxed version is used in their case study. In light of the compact transport model in [9], [13] and detailed flexible truck routing model in [14], we formulate a simplified flexible truck routing model that can model tank storage flexibility and time delay. (2) For pipeline transportation, detailed modeling that considers flow-pressure relations in [10] may not be computationally tractable for planning problems. Thus, a simplified linear model is used in this paper. (3) For hydrogen storage facilities, as they are usually used for seasonal storage purposes, chronological simulations are important to capture storage behaviors. Limited to the computational capability, most works use representative days or weeks to construct future scenarios in planning problems.

However, traditional pumped storage or battery storage models [16], [17], which are formulated on a daily or weekly recycle basis, are used for hydrogen modeling in most literature. To tackle this storage modeling challenge, based on representative week settings, a hydrogen storage model that can estimate annual capacity requirement is proposed in this work.

The contributions of this work include:

- We formulate novel deterministic hydrogen transportation and storage models, in detail, a simplified truck routing model that can reflect tank storage flexibility, and a seasonal storage model that can estimate annual capacity requirement with representative weeks.
- We propose a joint planning approach for power transmission and hydrogen transportation networks, which can achieve resource complementation and address various uncertainties. Through numerical simulations, we found our proposed joint planning approach has benefits in saving total system cost, reducing renewable energy curtailment, and increasing the utilization level of transmission lines.

## II. HYDROGEN TRANSPORTATION AND STORAGE

Flexible truck routing, pipeline transportation, and representative week based seasonal storage formulations are presented in this section.

### A. Truck Transportation Network

The hydrogen quantity in charged and empty trucks in each zone changes according to leaving and arriving schedules as well as charging and discharging behaviors of trucks, as shown in Fig. 2. Equation (1a) models how the hydrogen quantity in charged trucks changes considering the aforementioned behaviors. We use  $e_{k,z,s,d}^{\text{tr}}$  to represent hydrogen quantity in charged trucks with transportation technology  $k$  in zone  $z$  at the end of day  $d$  in scenario  $s$ . Travel time delay has been taken into account in (1a). If charged trucks with  $q_{k,m,n,s,d}^{\text{tr}}$  hydrogen quantity leave at the end of day  $d$  from zone  $m$  to zone  $n$ , when accounting a time delay of  $T_{k,m,n}$  days, we

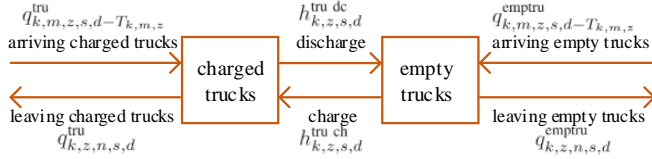


Fig. 2. Illustration of truck modeling.

have the same quantity of hydrogen arriving in zone  $n$  at the beginning of day  $d+T_{k,m,n}$ . Note (1a) can be simplified to the classical transport model that considers time delay by letting  $e_{k,z,s,d}^{\text{tru}} = 0$ .

$$e_{k,z,s,d}^{\text{tru}} = e_{k,z,s,d-1}^{\text{tru}} + \sum_{m|(m,z) \in \mathcal{R}} q_{k,m,z,s,d-T_{k,m,z}}^{\text{tru}} + h_{k,z,s,d}^{\text{tru ch}} - h_{k,z,s,d}^{\text{tru dc}} - \sum_{n|(z,n) \in \mathcal{R}} q_{k,z,n,s,d}^{\text{tru}} \quad \forall k \in \mathcal{K}^{\text{tru}}, z \in \mathcal{Z}, s \in \mathcal{S}, d \in \mathcal{TD}_s \quad (1a)$$

Empty trucks can also be transported between any two zones. Analogously, the transportation of empty capacity can be modeled in (1b).

$$e_{k,z,s,d}^{\text{emptru}} = e_{k,z,s,d-1}^{\text{emptru}} + \sum_{m|(m,z) \in \mathcal{R}} q_{k,m,z,s,d-T_{k,m,z}}^{\text{emptru}} - h_{k,z,s,d}^{\text{tru ch}} + h_{k,z,s,d}^{\text{tru dc}} - \sum_{n|(z,n) \in \mathcal{R}} q_{k,z,n,s,d}^{\text{emptru}} \quad \forall k \in \mathcal{K}^{\text{tru}}, z \in \mathcal{Z}, s \in \mathcal{S}, d \in \mathcal{TD}_s \quad (1b)$$

The hydrogen quantities and carrying capacities are non-negative, which are shown in (1c) and (1d).

$$0 \leq q_{k,m,n,s,d}^{\text{tru}}, \quad 0 \leq q_{k,m,n,s,d}^{\text{emptru}} \quad \forall k \in \mathcal{K}^{\text{tru}}, (m,n) \in \mathcal{R}, s \in \mathcal{S}, d \in \mathcal{TD}_s \quad (1c)$$

$$0 \leq e_{k,z,s,d}^{\text{tru}}, \quad 0 \leq e_{k,z,s,d}^{\text{emptru}} \quad \forall k \in \mathcal{K}^{\text{tru}}, z \in \mathcal{Z}, s \in \mathcal{S}, d \in \mathcal{TD}_s \quad (1d)$$

Limited by compression or liquefaction capacities, bounds for charge quantity are shown in (1e).

$$0 \leq h_{k,z,s,d}^{\text{tru ch}} \leq \bar{H}_{k,z}^{\text{tru}}, \quad 0 \leq h_{k,z,s,d}^{\text{tru dc}} \quad \forall k \in \mathcal{K}^{\text{tru}}, z \in \mathcal{Z}, s \in \mathcal{S}, d \in \mathcal{TD}_s \quad (1e)$$

The total amount of full and empty truck capacity in all zone during day  $d$  can be calculated in two ways: (1) the total amount staying in all zone at the end of the previous day plus the amount just arrived at the beginning of day  $d$ , which is  $\sum_{z \in \mathcal{Z}} [e_{k,z,s,d-1}^{\text{tru}} + e_{k,z,s,d-1}^{\text{emptru}} + \sum_{m \in \mathcal{Z} \setminus z} (q_{k,m,z,s,d-T_{k,m,z}}^{\text{tru}} + q_{k,m,z,s,d-T_{k,m,z}}^{\text{emptru}})]$ . Considering  $\sum_{z \in \mathcal{Z}} \sum_{m \in \mathcal{Z} \setminus z} (q_{k,m,z,s,d-T_{k,m,z}}^{\text{tru}} + q_{k,m,z,s,d-T_{k,m,z}}^{\text{emptru}}) = \sum_{(m,n) \in \mathcal{R}} (q_{k,m,n,s,d-T_{k,m,n}}^{\text{tru}} + q_{k,m,n,s,d-T_{k,m,n}}^{\text{emptru}})$ , the amount can be further represented as  $\sum_{z \in \mathcal{Z}} (e_{k,z,s,d-1}^{\text{tru}} + e_{k,z,s,d-1}^{\text{emptru}}) + \sum_{(m,n) \in \mathcal{R}} (q_{k,m,n,s,d-T_{k,m,n}}^{\text{tru}} + q_{k,m,n,s,d-T_{k,m,n}}^{\text{emptru}})$ . (2) the total amount staying in all zone at the end of day  $d$  plus the amount departed at the end of day  $d$ . In a similar manner to rearrange the formula, we have  $\sum_{z \in \mathcal{Z}} (e_{k,z,s,d}^{\text{tru}} + e_{k,z,s,d}^{\text{emptru}}) + \sum_{(m,n) \in \mathcal{R}} (q_{k,m,n,s,d}^{\text{tru}} + q_{k,m,n,s,d}^{\text{emptru}})$ . These two representations

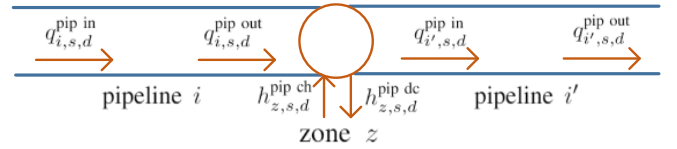


Fig. 3. Illustration of pipeline modeling.

are equivalent, which can be inferred from (1a) and (1b) by adding them up.

The hydrogen quantity and empty truck capacity that are in transit during the whole day of  $d$  can be represented by  $\sum_{(m,n) \in \mathcal{R}} \sum_{\delta=d-T_{k,m,n}+1}^{d-1} q_{k,m,n,s,\delta}^{\text{tru}}$  and  $\sum_{(m,n) \in \mathcal{R}} \sum_{\delta=d-T_{k,m,n}+1}^{d-1} q_{k,m,n,s,\delta}^{\text{emptru}}$  for each truck technology  $k$ , respectively. Note just departed and arrived trucks are not taken into account.

Finally, by summing up the in transit and in zone amounts, the total capacity for hydrogen truck technology  $k$  in each day is limited by  $\bar{Q}_k$  in (1f) or (1g).

$$\sum_{(m,n) \in \mathcal{R}} \sum_{\delta=d-T_{k,m,n}}^{d-1} (q_{k,m,n,s,\delta}^{\text{tru}} + q_{k,m,n,s,\delta}^{\text{emptru}}) + \sum_{z \in \mathcal{Z}} (e_{k,z,s,d-1}^{\text{tru}} + e_{k,z,s,d-1}^{\text{emptru}}) \leq \bar{Q}_k \quad \forall k \in \mathcal{K}^{\text{tru}}, s \in \mathcal{S}, d \in \mathcal{TD}_s \quad (1f)$$

$$\sum_{(m,n) \in \mathcal{R}} \sum_{\delta=d-T_{k,m,n}+1}^d (q_{k,m,n,s,\delta}^{\text{tru}} + q_{k,m,n,s,\delta}^{\text{emptru}}) + \sum_{z \in \mathcal{Z}} (e_{k,z,s,d-1}^{\text{tru}} + e_{k,z,s,d-1}^{\text{emptru}}) \leq \bar{Q}_k \quad \forall k \in \mathcal{K}^{\text{tru}}, s \in \mathcal{S}, d \in \mathcal{TD}_s \quad (1g)$$

Hydrogen quantity stored in truck tanks is assumed to recycle in each representative week. The main purpose is to tackle hydrogen generation and demand mismatch during a few days. Truck tank storage is not used as seasonal storage, as seasonal storage usage may limit the mobility of trucks. Thus, recycle conditions for truck tank storage are modeled in (1h).

$$e_{k,z,s,|\mathcal{TD}_s|}^{\text{tru}} = e_{k,z,s,0}^{\text{tru}} \quad \forall k \in \mathcal{K}^{\text{tru}}, z \in \mathcal{Z}, s \in \mathcal{S} \quad (1h)$$

## B. Pipeline Network

To keep the whole formulation tractable, we use a simplified pipeline model, which is similar to that in [14]. The net hydrogen flow to each zone  $z$ , i.e., the difference of bi-directional flows  $h_{z,s,d}^{\text{pip dc}} - h_{z,s,d}^{\text{pip ch}}$ , equals to total flow from connected pipelines as shown in Fig. 3. This flow balance constraint is modeled in (2a). Both directional hydrogen flows from and to the pipeline network in each zone are bounded in (2b). If a pipeline is built, hydrogen flows at both ends of the pipeline are limited by line capacity; otherwise, these flows are zeros. We model this feature in (2c)-(2d). Linepack storage dynamics of each pipeline are presented in (2e). The state of charge (SOC) of line pack storage for each pipeline

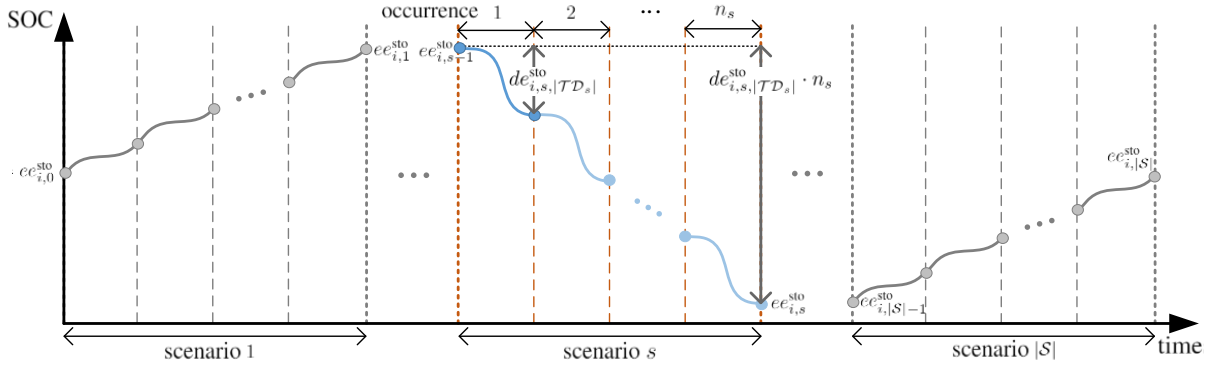


Fig. 4. Illustration of seasonal hydrogen storage modeling.

is limited by its capacity in (2f). In each scenario  $s$ , recycle conditions for linepack storage are presented in (2g).

$$h_{z,s,d}^{\text{pip dc}} - h_{z,s,d}^{\text{pip ch}} = \sum_{i|i=(m,z) \in \mathcal{P}} q_{i,s,d}^{\text{pip out}} - \sum_{i|i=(z,n) \in \mathcal{P}} q_{i,s,d}^{\text{pip in}} \quad \forall z \in \mathcal{Z}, s \in \mathcal{S}, d \in \mathcal{TD}_s \quad (2a)$$

$$0 \leq h_{z,s,d}^{\text{pip ch}} \leq NT^{\text{day}} \cdot \bar{H}_z^{\text{pip}}, \quad 0 \leq h_{z,s,d}^{\text{pip dc}} \leq NT^{\text{day}} \cdot \bar{H}_z^{\text{pip}} \quad \forall z \in \mathcal{Z}, s \in \mathcal{S}, d \in \mathcal{TD}_s \quad (2b)$$

$$-\bar{P}_i^{\text{pip}} \cdot NT^{\text{day}} \cdot w_i \leq q_{i,s,d}^{\text{pip in}} \leq \bar{P}_i^{\text{pip}} \cdot NT^{\text{day}} \cdot w_i \quad \forall i \in \mathcal{P}, s \in \mathcal{S}, d \in \mathcal{TD}_s \quad (2c)$$

$$-\bar{P}_i^{\text{pip}} \cdot NT^{\text{day}} \cdot w_i \leq q_{i,s,d}^{\text{pip out}} \leq \bar{P}_i^{\text{pip}} \cdot NT^{\text{day}} \cdot w_i \quad \forall i \in \mathcal{P}, s \in \mathcal{S}, d \in \mathcal{TD}_s \quad (2d)$$

$$e_{i,s,d}^{\text{pip}} = e_{i,s,d-1}^{\text{pip}} + q_{i,s,d}^{\text{pip in}} - q_{i,s,d}^{\text{pip out}} \quad \forall i \in \mathcal{P}, s \in \mathcal{S}, d \in \mathcal{TD}_s \quad (2e)$$

$$0 \leq e_{i,s,d}^{\text{pip}} \leq \bar{E}_i^{\text{pip}} \cdot w_i \quad \forall i \in \mathcal{P}, s \in \mathcal{S}, d \in \mathcal{TD}_s \quad (2f)$$

$$e_{i,s,|\mathcal{TD}_s|}^{\text{pip}} = e_{i,s,0}^{\text{pip}} \quad \forall i \in \mathcal{P}, s \in \mathcal{S} \quad (2g)$$

### C. Hydrogen Storage

Conventional electric storage, such as pumped storage and battery storage [16], [17], are usually operated in daily or weekly cycles. Thus, a storage cycle can be fully covered in representative day or week settings. In each storage cycle, time periods are sequential and uninterrupted. Given seasonal storage purposes and representative week settings in this work, hydrogen storage modeling should be reformulated. As shown in Fig. 4, representative week scenarios are labeled by indices  $s = 1, 2, \dots, |\mathcal{S}|$ , which are listed in chronological order. For each scenario  $s$ ,  $n_s$  times of sequential occurrence are considered to reflect annual dynamics of hydrogen storage.

Inside each scenario, the deviation of state of charge (SOC) from initial SOC in this scenario, which is denoted by  $de_{i,s,d}^{\text{sto}}$ , is calculated in (3a) for all time periods. As the compression is usually needed to store hydrogen in physical-based storage, capacities of planned compressors are limited in (3b). The initial SOC deviations  $de_{i,s,0}^{\text{sto}}$  are trivially assigned to zero in (3c). The upper and lower bounds for SOC in all the occurrences of each scenario are modeled in (3d)-(3e) and (3f)-(3g), respectively.

Given the end SOC in the last occurrence of scenario  $s-1$  is the initial SOC of scenario  $s$ , the end SOC changes between

consecutive scenarios can be represented in (3h) by assuming the pattern in scenario  $s$  would sequentially repeat  $n_s$  times. The initial SOC  $ee_{i,0}^{\text{sto}}$  is defined in (3i). Used for seasonal storage purpose, hydrogen storage has a recycle condition as modeled in (3j).

$$de_{i,s,d}^{\text{sto}} = de_{i,s,d-1}^{\text{sto}} + h_{i,s,d}^{\text{sto ch}} - h_{i,s,d}^{\text{sto dc}} \quad \forall i \in \mathcal{E}, s \in \mathcal{S}, d \in \mathcal{TD}_s \quad (3a)$$

$$0 \leq h_{i,s,d}^{\text{sto ch}} \leq NT^{\text{day}} \cdot \bar{H}_i^{\text{sto}}, \quad 0 \leq h_{i,s,d}^{\text{sto dc}} \leq NT^{\text{day}} \cdot \bar{H}_i^{\text{sto}} \quad \forall i \in \mathcal{E}, s \in \mathcal{S}, d \in \mathcal{TD}_s \quad (3b)$$

$$de_{i,s,0}^{\text{sto}} = 0 \quad \forall i \in \mathcal{E}, s \in \mathcal{S} \quad (3c)$$

$$ee_{i,s-1}^{\text{sto}} + de_{i,s,d}^{\text{sto}} \leq \bar{\gamma}_i \cdot \bar{E}_i^{\text{sto}} \quad \forall i \in \mathcal{E}, s \in \mathcal{S}, d \in \mathcal{TD}_s \quad (3d)$$

$$ee_{i,s-1}^{\text{sto}} + de_{i,s,|\mathcal{TD}_s|}^{\text{sto}} \cdot (n_s - 1) + de_{i,s,d}^{\text{sto}} \leq \bar{\gamma}_i \cdot \bar{E}_i^{\text{sto}} \quad \forall i \in \mathcal{E}, s \in \mathcal{S}, d \in \mathcal{TD}_s \quad (3e)$$

$$ee_{i,s-1}^{\text{sto}} + de_{i,s,d}^{\text{sto}} \geq \underline{\gamma}_i \cdot \bar{E}_i^{\text{sto}} \quad \forall i \in \mathcal{E}, s \in \mathcal{S}, d \in \mathcal{TD}_s \quad (3f)$$

$$ee_{i,s-1}^{\text{sto}} + de_{i,s,|\mathcal{TD}_s|}^{\text{sto}} \cdot (n_s - 1) + de_{i,s,d}^{\text{sto}} \geq \underline{\gamma}_i \cdot \bar{E}_i^{\text{sto}} \quad \forall i \in \mathcal{E}, s \in \mathcal{S}, d \in \mathcal{TD}_s \quad (3g)$$

$$ee_{i,s}^{\text{sto}} = ee_{i,s-1}^{\text{sto}} + de_{i,s,|\mathcal{TD}_s|}^{\text{sto}} \cdot n_s \quad \forall i \in \mathcal{E}, s \in \mathcal{S} \quad (3h)$$

$$ee_{i,0}^{\text{sto}} = \gamma_i^0 \cdot \bar{E}_i^{\text{sto}} \quad \forall i \in \mathcal{E} \quad (3i)$$

$$ee_{i,|\mathcal{S}|}^{\text{sto}} = ee_{i,0}^{\text{sto}} \quad \forall i \in \mathcal{E} \quad (3j)$$

## III. DETERMINISTIC JOINT PLANNING MODEL

In this section, we demonstrate a modeling framework over two timescales, and a deterministic joint planning formulation for power transmission and hydrogen transportation networks.

### A. Two-Timescale Modeling Framework

As both power and hydrogen systems are incorporated in our proposed planning approach, system components with

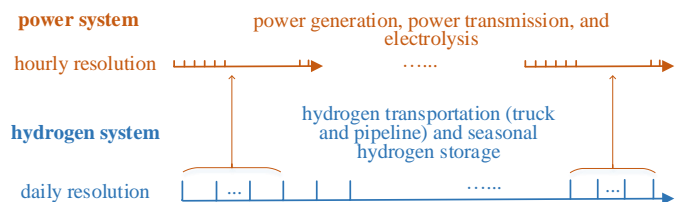


Fig. 5. Timescales in the optimization problem.

distinctive physical characteristics need to be modeled in different time scales. In hydrogen systems, hydrogen storage usually has seasonal cycles, and truck transportation takes a few days to travel between two zones. In power systems, steady-state models in planning problems usually have an hourly resolution, as electric demand and renewable energy output fluctuate in a relatively short time frame.

Thus, different resolutions are applied for resources with different timescales in our optimization, as shown in Fig. 5. In detail, hydrogen system components are modeled in daily resolution (with time periods  $d \in \mathcal{TD}_s$ ), while power system components are modeled in hourly resolution (with time periods  $t \in \mathcal{TH}_s$ ).

### B. Other Constraints for Hydrogen Supply Chain

In addition to the hydrogen transportation and storage modeling in section II, other constraints for hydrogen quantity balance and hydrogen productions in hydrogen supply chains are established in this subsection. Considering hydrogen production and demand in each zone  $z$  as well as truck and pipeline transportation among zones, in (4a), zonal hydrogen quantity balance constraints are presented. Hydrogen production limits for steam methane reformers and electrolyzers are presented in (4b) and (4c) with respective investment decisions. The conversion efficiency between electric power and hydrogen is modeled as  $\phi_i$  in (4c).

$$\begin{aligned} & \sum_{i \in \mathcal{HR}_z} h_{i,s,d} + \sum_{i \in \mathcal{HE}_z} \sum_{t \in \mathcal{TH}_{s,d}} \phi_i \cdot p_{i,s,t} + \sum_{\forall i \in \mathcal{E}_z} (h_{i,s,d}^{\text{sto dc}} \\ & - h_{i,s,d}^{\text{sto ch}}) + \sum_{\forall k \in \mathcal{K}^{\text{tru}}} (h_{k,z,s,d}^{\text{tru dc}} - h_{k,z,s,d}^{\text{tru ch}}) - \\ & \sum_{i|z=(z,n) \in \mathcal{P}} q_{i,s,d}^{\text{pip in}} + \sum_{i|(m,z) \in \mathcal{P}} q_{i,s,d}^{\text{pip out}} = D_{z,s,d}^{\text{hyd}} \\ & \forall z \in \mathcal{Z}, s \in \mathcal{S}, d \in \mathcal{TD}_s \quad (4a) \\ & 0 \leq h_{i,s,d} \leq NT^{\text{day}} \cdot \bar{H}_i \quad \forall i \in \mathcal{HR}, s \in \mathcal{S}, d \in \mathcal{TD}_s \quad (4b) \\ & 0 \leq \phi_i \cdot p_{i,s,t} \leq \bar{H}_i \quad \forall i \in \mathcal{HE}, s \in \mathcal{S}, t \in \mathcal{TH}_s \quad (4c) \end{aligned}$$

### C. Constraints for Power Transmission Expansion Planning

Power system transmission expansion planning is formulated in (5). For each bus, an electric power balance constraint is described in (5a). Limits for renewable power output are modeled in (5b). For conventional generators, power output and ramp rate are limited in (5c) and (5d), respectively. For existing transmission lines, branch flow is calculated in (5e) through the direct current power flow (DCPF) approach, and bounded in (5f). For candidate lines, a disjunctive model [18] is used to formulate the flow-angle relations and flow limits in (5g) and (5h), respectively.

$$\begin{aligned} & \sum_{i|(m,b) \in \mathcal{L} \cup \mathcal{L}^e} f_{i,s,t} - \sum_{i|(b,n) \in \mathcal{L} \cup \mathcal{L}^e} f_{i,s,t} + \sum_{i \in \mathcal{G}_b} p_{i,s,t} \\ & + \sum_{i \in \mathcal{W}_b} (W_{i,s,t} - wc_{i,s,t}) = \sum_{i \in \mathcal{D}_b} D_{i,s,t}^{\text{le}} + \sum_{i \in \mathcal{HE}_b} p_{i,s,t} \\ & \forall b \in \mathcal{B}, s \in \mathcal{S}, t \in \mathcal{TH}_s \quad (5a) \end{aligned}$$

$$0 \leq wc_{i,s,t} \leq W_{i,s,t} \quad \forall i \in \mathcal{W}, s \in \mathcal{S}, t \in \mathcal{TH}_s \quad (5b)$$

$$\underline{P}_i \leq p_{i,s,t} \leq \bar{P}_i \quad \forall i \in \mathcal{G}, s \in \mathcal{S}, t \in \mathcal{TH}_s \quad (5c)$$

$$-RD_i \leq p_{i,s,t+1} - p_{i,s,t} \leq RU_i \quad \forall i \in \mathcal{G}, s \in \mathcal{S}, t \in \mathcal{TH}_s \quad (5d)$$

$$\begin{aligned} f_{i,s,t} &= (\theta_{m,s,t} - \theta_{n,s,t})/x_i \\ \forall i &= (m,n) \in \mathcal{L}^e, s \in \mathcal{S}, t \in \mathcal{TH}_s \quad (5e) \end{aligned}$$

$$-F_i \leq f_{i,s,t} \leq F_i \quad \forall i \in \mathcal{L}^e, s \in \mathcal{S}, t \in \mathcal{TH}_s \quad (5f)$$

$$\begin{aligned} f_{i,s,t} - (\theta_{m,s,t} - \theta_{n,s,t})/x_i + M \cdot z_i &\leq M, \\ -f_{i,s,t} + (\theta_{m,s,t} - \theta_{n,s,t})/x_i + M \cdot z_i &\leq M \\ \forall i &= (m,n) \in \mathcal{L}, s \in \mathcal{S}, t \in \mathcal{TH}_s \quad (5g) \end{aligned}$$

$$-F_i \cdot z_i \leq f_{i,s,t} \leq F_i \cdot z_i \quad \forall i \in \mathcal{L}, s \in \mathcal{S}, t \in \mathcal{TH}_s \quad (5h)$$

### D. Deterministic Problem Formulation

Finally, the proposed joint planning is formulated in (6), wherein the objective function is the sum of the investment and operation cost for truck (terms a1-a3) and pipeline (term b) hydrogen transportation, hydrogen production (terms c1-c2), hydrogen storage (terms d1-d2), as well as electric power generation and transmission (terms e1-e2).

$$\min \quad \text{obj} \quad (6a)$$

$$\text{s.t.} \quad (1a)-(1e), (1f)(\text{or } (1g)), (1h), (2)-(5) \quad (6b)$$

where,

$$\begin{aligned} \text{obj} &= \underbrace{\sum_{k \in \mathcal{K}^{\text{tru}}} \left( ICQ_k^{\text{tru}} \cdot \bar{Q}_k + \sum_{z \in \mathcal{Z}} ICH_{k,z}^{\text{tru}} \cdot \bar{H}_{k,z}^{\text{tru}} \right)}_{\text{term a1}} \\ &+ \underbrace{\sum_{k \in \mathcal{K}^{\text{tru}}} \sum_{(m,n) \in \mathcal{R}} \sum_{s \in \mathcal{S}} \sum_{d \in \mathcal{TD}_s} n_s \cdot OC_{k,m,n}^{\text{tru}} \cdot q_{k,m,n,s,d}^{\text{tru}}}_{\text{term a2}} \\ &+ \underbrace{\sum_{k \in \mathcal{K}^{\text{tru}}} \sum_{(m,n) \in \mathcal{R}} \sum_{s \in \mathcal{S}} \sum_{d \in \mathcal{TD}_s} n_s \cdot OC_{k,m,n}^{\text{emptru}} \cdot q_{k,m,n,s,d}^{\text{emptru}}}_{\text{term a3}} \\ &+ \underbrace{\sum_{i \in \mathcal{P}} IC_i^{\text{pip}} \cdot w_i + \sum_{z \in \mathcal{Z}} ICH_z^{\text{pip}} \cdot \bar{H}_z^{\text{pip}}}_{\text{term b}} \\ &+ \underbrace{\sum_{i \in \mathcal{HE} \cup \mathcal{HR}} ICH_i^{\text{prd}} \cdot \bar{H}_i}_{\text{term c1}} + \underbrace{\sum_{i \in \mathcal{HR}} \sum_{s \in \mathcal{S}} \sum_{d \in \mathcal{TD}_s} n_s \cdot OC_i^{\text{prd}} \cdot h_{i,s,d}}_{\text{term c2}} \\ &+ \underbrace{\sum_{i \in \mathcal{E}} \left( ICE_i^{\text{sto}} \cdot \bar{E}_i + ICH_i^{\text{sto}} \cdot \bar{H}_i^{\text{sto}} \right)}_{\text{term d1}} \\ &+ \underbrace{\sum_{i \in \mathcal{E}} \sum_{s \in \mathcal{S}} \sum_{d \in \mathcal{TD}_s} n_s \cdot \left( OC_i^{\text{sto ch}} \cdot h_{i,s,d}^{\text{sto ch}} + OC_i^{\text{sto dc}} \cdot h_{i,s,d}^{\text{sto dc}} \right)}_{\text{term d2}} \\ &+ \underbrace{\sum_{i \in \mathcal{L}^e} IC_i^{\text{line}} \cdot z_i}_{\text{term e1}} + \underbrace{\sum_{i \in \mathcal{G}} \sum_{s \in \mathcal{S}} \sum_{t \in \mathcal{TH}_s} n_s \cdot OC_i^{\text{pgen}} \cdot p_{i,s,t}}_{\text{term e2}} \quad (6c) \end{aligned}$$

## IV. JOINT PLANNING UNDER UNCERTAINTY

The renewable energy profile used in the joint planning model is usually generated from historical power output or meteorological measurements, which may not necessarily guarantee system operational feasibility in some extreme conditions.

We use a robust joint planning approach to enhance future operational adequacy.

### A. Robust Joint Planning Approach

The deterministic planning model in (6) is abstractly expressed in (7). Objective function in (7a) corresponds to that in (6a). The constraints related to investment decision variables only are represented in (7b), and (7c) includes all the operational constraints.  $x$  is a vector for planning decisions  $z_i$ ,  $\overline{H}_i$ ,  $\overline{Q}_k$ ,  $\overline{H}_{k,z}^{\text{tru}}$ ,  $w_i$ ,  $\overline{H}_z^{\text{pip}}$ ,  $\overline{E}_i^{\text{sto}}$ ,  $\overline{H}_i^{\text{sto}}$ . While  $y$  is a vector for operational decisions. Vector  $\hat{u}$  contains variables for renewable power  $W_{i,s,t}$ , electric load  $D_{i,s,t}^{\text{ele}}$ , and hydrogen demand  $D_{z,s,d}^{\text{hyd}}$ . We treat  $\hat{u}$  as a constant vector in the deterministic planning model.

$$\min_{x,y} a^\top x + b^\top y \quad (7a)$$

$$\text{s.t.} \quad Ax \leq c \quad (7b)$$

$$Bx + Cy \leq g + G\hat{u} \quad (7c)$$

Taking  $u$  as uncertain variables, we apply a robust optimization formulation to our joint planning problem. The annual operational cost is still estimated for the given deterministic profile  $\hat{u}$ . As extreme cases may not happen everyday, it's improper to use them to estimate the annual operational cost. In (8), our formulation guarantees the system operational feasibility if  $u$  is in a predefined uncertainty set  $U$ . As shown in (8a), the objective function gives priority to investment decisions that can handle all possible uncertainty realizations in  $U$ . The deterministic constrains are kept in (8b)-(8c) of the robust formulation to estimate annual operational cost. Operational constraints for robust optimization are defined in (8d)-(8e), which are relaxed by non-negative variables  $\sigma$  to avoid numerical infeasibility. In detailed, a term  $\sigma_{z,s,d}^{\text{h}+} - \sigma_{z,s,d}^{\text{h}-}$  is added to the left-hand-side (LHS) of hydrogen balance constraints (4a); similarly,  $\sigma_{b,s,t}^{\text{e}+} - \sigma_{b,s,t}^{\text{e}-}$  is added to the LHS of electricity balance constraints (5a). The vector  $\sigma$  contains all slack variables of  $\sigma_{z,s,d}^{\text{h}+}$ ,  $\sigma_{z,s,d}^{\text{h}-}$ ,  $\sigma_{b,s,t}^{\text{e}+}$ , and  $\sigma_{b,s,t}^{\text{e}-}$ , which are non-negative as shown in (8e).

$$\min_{x,y} a^\top x + b^\top y + M \cdot \max_{u \in U} \min_{y(u), \sigma(u)} \mathbf{1}^\top \sigma(u) \quad (8a)$$

$$\text{s.t.} \quad Ax \leq c \quad (8b)$$

$$Bx + Cy \leq g + G\hat{u} \quad (8c)$$

$$Bx + Cy(u) \leq g + Gu + K\sigma(u) : \lambda \quad (8d)$$

$$\mathbf{0} \leq \sigma(u) \quad (8e)$$

### B. C&CG Algorithm

A column-and-constraint generation algorithm [15] is used to solve the robust optimization problem in (8). The algorithm decomposes (8) into a master problem in (9) and a sub problem in (10). The master and sub problems offer lower and upper bound for the problem in (8), respectively. They are solved

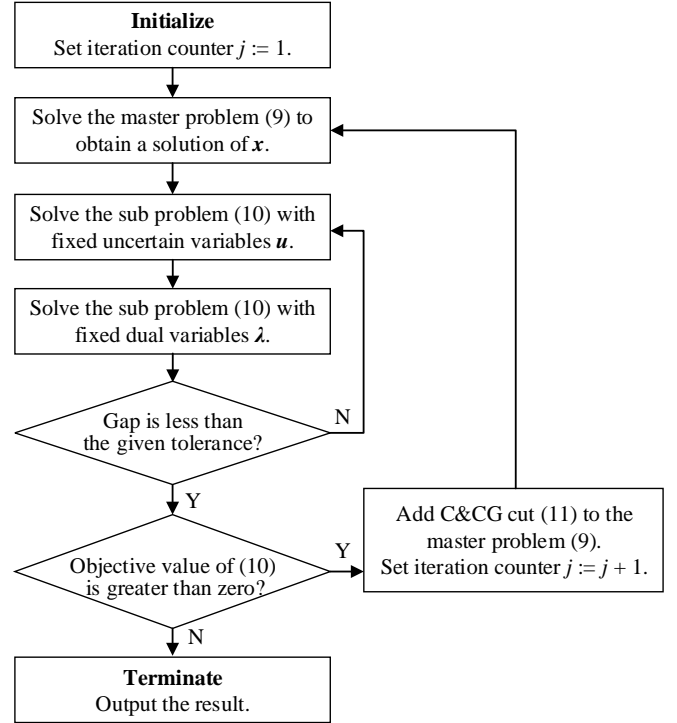


Fig. 6. Flowchart of the C&CG algorithm.

iteratively until the gap between upper and lower bounds shrinks below a predefined threshold.

$$\text{(MP)} \quad \min_{x,y} a^\top x + b^\top y \quad (9a)$$

$$\text{s.t.} \quad Ax \leq c \quad (9b)$$

$$Bx + Cy \leq g + G\hat{u} \quad (9c)$$

$$\text{C\&CG cuts} \quad (9d)$$

$$\text{(SP)} \quad \max_{u,\lambda} (g + Gu - B\hat{x})^\top \lambda \quad (10a)$$

$$\text{s.t.} \quad \lambda^\top C = \mathbf{0}^\top : y(u) \quad (10b)$$

$$\lambda^\top K \leq \mathbf{1}^\top : \sigma(u) \quad (10c)$$

$$\lambda \leq \mathbf{0} \quad (10d)$$

$$u \in U \quad (10e)$$

Although the bilinear sub problem in (10) can be equivalently transformed to a mixed-integer linear program (MILP) [19], this suffers from high computational burdens. We use a tractable heuristic alternating direction method [19], [20] to solve (10). When either  $u$  or  $\lambda$  is fixed, (10) becomes a linear program (LP) problem. The two LP problems are iteratively solved until obtaining a small enough gap between two objective values. In each iteration, if the objective of (10) is greater than zero, which means the operational problem is infeasible under the worst-case uncertainty realization, a C&CG cut (11) is added to the master problem (9). In (11),  $\hat{u}^{(j)}$  is the optimal solution of (10) in each iteration  $j$ . The procedure of this algorithm is shown in Fig. 6.

$$Bx + Cy^{(j)} \leq g + G\hat{u}^{(j)} \quad (11)$$

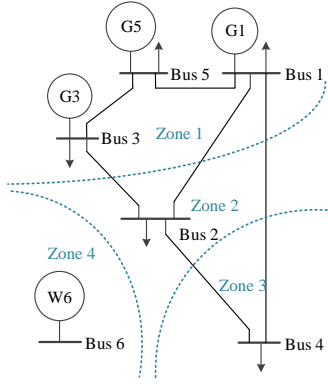


Fig. 7. Extended Garver's 6 bus system.

## V. CASE STUDY

We use extended Garver's 6 bus and IEEE 118 bus systems to demonstrate the advantages of our proposed joint planning approach. All the MILP and LP problems were solved by using Cplex 12.10 [21] on a computer with Intel Core i7-9700 CPU and 64 GB RAM.

### A. Garver's 6 Bus System

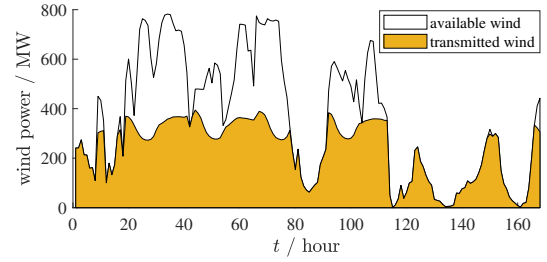
To study the role of the hydrogen supply chain in transmission expansion plannings, the Garver's 6 bus system in [22] is extended in this article. The system topology is shown in Fig. 7. The power system contains six buses, six existing transmission lines, three conventional generators, and a wind farm. The hydrogen supply system is expected to be planned given candidate hydrogen production units, hydrogen transportation infrastructures, and hydrogen storage. A representative week scenario is incorporated in the formulation for each quarter in a year.

1) *Value of the Proposed Joint Planning:* We compare our proposed joint planning model with a separate model, which makes investment decisions for the power transmission system and the hydrogen transportation system separately without considering candidate electrolyzer units. The separate planning model in fact ignores the coupling between these two systems. Table I shows the planning result comparison for the joint and separate models. As indicated, the joint planning has benefits in reducing the overall annualized investment and operational

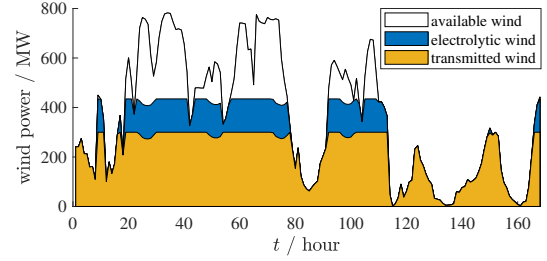
TABLE I  
PLANNING RESULT FOR EXTENDED GARVER'S 6 BUS SYSTEM

model	planning decision		annualized total cost ( $10^6$ \$)
	transmission	hydrogen supply chain	
joint planning	line 2-6 $\times$ 3 line 2-3 $\times$ 2	electrolyzer (2.54 ton/h in Z4) steam reformer (2.35 ton/h in Z3, 2.88 ton/h in Z4) storage (34.44 ton, 1.44 ton/h in Z3, 47.01 ton, 1.96 ton/h in Z4) liquid truck (1165.14 ton)	114.57
		steam reformer (2.64 ton/h in Z3, 4.67 ton/h in Z4) storage (112.05 ton, 4.67 ton/h in Z4) liquid truck (1165.14 ton)	
separate planning	line 2-6 $\times$ 4 line 2-3 $\times$ 2	steam reformer (2.64 ton/h in Z3, 4.67 ton/h in Z4) storage (112.05 ton, 4.67 ton/h in Z4) liquid truck (1165.14 ton)	115.94

\* Z1-Z4 in the table represent zone 1-zone 4.



(a)



(b)

Fig. 8. Comparison of wind power and transmission lines utilization in the quarter-1 scenario: (a) separate planning, (b) joint planning.

cost in comparison to the separate model. To address the deliverability and/or congestion issues that happen in the peak wind power periods at bus 6, four transmission lines that connect to bus 6 are planned in the separate model solution. This can avoid massive wind curtailment when the wind power output is large. From the perspective of integrated power and hydrogen system, electrolyzer provides an alternative option to relieve such deliverability and/or congestion issues through converting wind power to hydrogen to serve the hydrogen loads. In this way, electrolyzer investment can potentially reduce the transmission line construction. As shown in our joint planning result, one transmission line construction is avoided compared to the separate planning model.

In the separate model, the annual wind curtailment of the wind farm at bus 6 is  $4.86 \times 10^5$  MWh. Although constructing one less exporting transmission line from bus 6, the joint planning model enables a reduced annual wind curtailment of  $2.97 \times 10^5$  MWh. The wind energy utilization level of the wind farm at bus 6 also increases from 77.05% to 85.99% with the joint planning model. As an example, Fig. 8 shows the available and actual generated wind power in a representative week scenario in quarter 1 (i.e., January to March). Under the investment decision from the joint planning, as indicated, more wind energy can be utilized during the peak periods, thus wind power curtailment can be reduced.

In terms of transmission lines in the corridor 2-6, due to the volatility of wind output at bus 6, the duration of base line-loading in a year is most likely larger than that of peak loading. Thus, more transmission lines would reduce the average utilization. The annual utilization level of 4 planned lines 2-6 in the separate planning model is 46.57%. While in the joint planning model, the utilization level of 3 planned transmission lines in the same corridor improves to 54.27%. In this case, converting part of peak wind power to hydrogen can

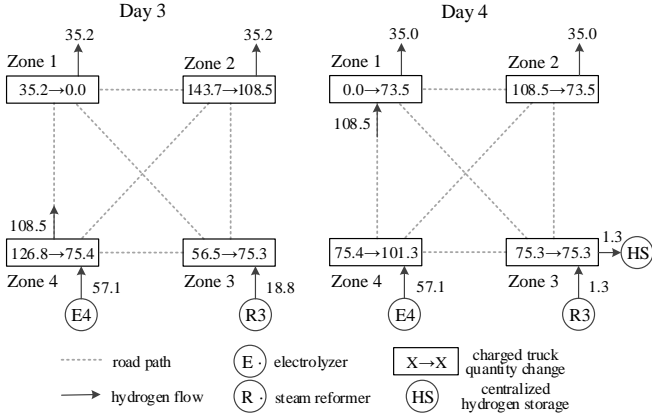


Fig. 9. An illustrative example for hydrogen mass flow in day 3 and day 4 of the quarter-1 weekly scenario (unit: ton)

reduce the number of planned transmission lines, thus improve the line utilization level. This analysis can also be indicated from the comparison in Fig. 8.

2) *Hydrogen System Modeling Illustration:* We use an illustrative example to show how our proposed truck routine model works. As shown in Fig. 9, we visualize the hydrogen quantity balance for each zone and flow changes in two daily time periods. In this example, hydrogen is transported from zone 4 to zone 1 by trucks, which leaves on day 3 and arrives on day 4 as delivery through this routine is assumed to arrive on the next day. Rectangular boxes in the figure show how hydrogen quantity in charged trucks changes over one day at each zone. As truck tanks can be used as storage devices in the hydrogen system, in zone 2, charged trucks gradually release the hydrogen quantity from previously arrived trucks in these two days. This simulation result shows that our proposed truck routing can reflect the short-term flexibility of truck tanks in the hydrogen supply chain.

To illustrate the modeling enhancement for seasonal hydrogen storage, we compare the proposed model with a model that assumes weekly recycle. The weekly cycle model is implemented by setting target SOC for each representative week scenario. The system planning result comparison is shown in Table II. As indicated, centralized hydrogen storage is not planned if the seasonal recycle feature is not modeled. Alternatively, the total planning capacities for steam reformers and electrolyzers are increased to address the peak hydrogen demand in the long term. Note this does not necessarily mean that storage is not required in the case with weekly cycle setting. The truck tank flexibility has been leveraged to deal with the short-term volatility in a week. Also, this study only models the cross zonal hydrogen transportation system. The need for storage in hydrogen distribution systems can be further investigated in the future, which is beyond the scope of this work. In summary, the proposed hydrogen storage model can reflect the seasonal cycling requirement in representative week settings while the traditional weekly cycle model cannot. This is the value of our proposed hydrogen storage model.

3) *Value of the Robust Planning:* Our proposed robust joint planning model in (8) is compared with a deterministic

TABLE II  
COMPARISON FOR HYDROGEN STORAGE MODEL IN EXTENDED GARVER'S 6 BUS SYSTEM

hydrogen storage model	total planning capacity		
	centralized hydrogen storage	steam reformer	electrolyzer
seasonal model (annual cycle)	81.45 ton, 81.45 ton/day	125.59 ton/day	60.98 ton/day
traditional model (weekly cycle)	0 ton, 0 ton/day	149.79 ton/day	64.46 ton/day

joint planning model, which is implemented by (6). Given an investment decision  $\hat{x}$  and a realization of uncertainty variable  $\hat{u}$ , we check the feasibility of the operational problem by solving (12), which uses the same abstract notations as the formulation in (8). The objective function of (12) evaluates the sum of imbalances at all the nodes in the power system and zones in the hydrogen supply chain.

$$\min_{y, \sigma} \mathbf{1}^\top \sigma \quad (12a)$$

$$B\hat{x} + Cy \leq g + G\hat{u} + K\sigma \quad (12b)$$

$$\mathbf{0} \leq \sigma \quad (12c)$$

The sampling method for possible realizations of uncertain variables  $\hat{u}$  in the uncertainty set is shown in (13). Given parameters  $\alpha^{\text{enl}}, \alpha^{\text{hl}} \in [0, 1]$ , electric net load without curtailment (denote as  $\text{enl}_{b,s,t} = \sum_{i \in \mathcal{D}_b} D_{i,s,t}^{\text{ele}} - \sum_{i \in \mathcal{W}_b} W_{i,s,t}$  for bus  $b$ ) and hydrogen load (denote as  $\text{hl}_{z,s,d} = D_{z,s,d}^{\text{hyd}}$  for zone  $z$ ) are sampled using (13a) and (13b), respectively.

$$\text{enl}_{b,s,t} = (1 - \alpha^{\text{enl}}) \cdot \underline{\text{enl}}_{b,s,t} + \alpha^{\text{enl}} \cdot \overline{\text{enl}}_{b,s,t} \quad \forall b \in \mathcal{B}, s \in \mathcal{S}, t \in \mathcal{TH}_s \quad (13a)$$

$$\text{hl}_{z,s,d} = (1 - \alpha^{\text{hl}}) \cdot \underline{\text{hl}}_{z,s,d} + \alpha^{\text{hl}} \cdot \overline{\text{hl}}_{z,s,d} \quad \forall z \in \mathcal{Z}, s \in \mathcal{S}, d \in \mathcal{TD}_s \quad (13b)$$

where,  $\underline{\text{enl}}_{b,s,t}$  ( $\underline{\text{hl}}_{z,s,t}$ ) and  $\overline{\text{enl}}_{b,s,t}$  ( $\overline{\text{hl}}_{z,s,t}$ ) are lower and upper bounds for  $\text{enl}_{b,s,t}$  ( $\text{hl}_{z,s,t}$ ), respectively.

The feasibility test results are shown in Fig. 10, wherein the sum of imbalances is from the objective value in (12a). As indicated, when electric net load and hydrogen load are high, the investment decision from the deterministic model suffers from imbalance issues, which would affect the system

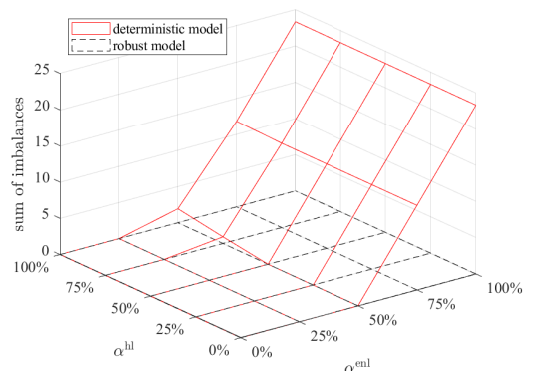


Fig. 10. Comparison of deterministic and robust approaches.

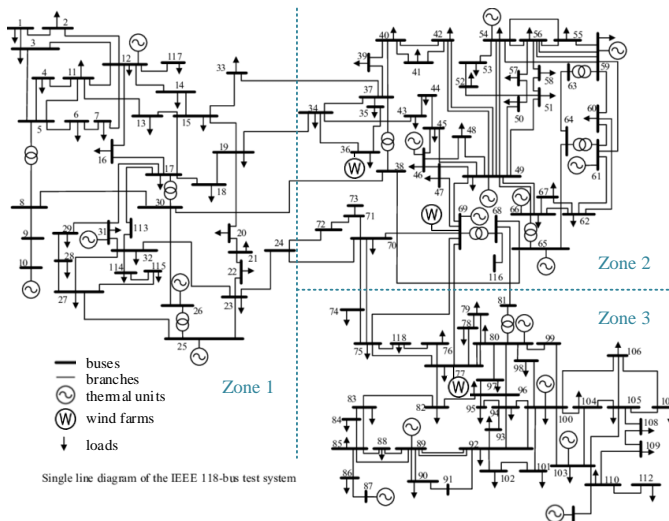


Fig. 11. Extended IEEE 118 bus system (the original figure is from [23]).

security in the operational phase. However, these imbalance issues are eliminated when we use the investment decision from the robust model. Thus, the robust joint planning model offers a solution that can hedge against the electric net load and hydrogen demand uncertainties.

### B. IEEE 118 Bus System

We also test the proposed joint planning approach in an extended IEEE 118 bus system. Numerical results with sensitivity analysis are presented.

1) *Case Settings and Results Summary*: The single line diagram for the power system part and the zoning setting for the hydrogen system part in the extended IEEE 118 bus system are shown in Fig. 11. The power system data settings are from [24]. Three wind farms are added at buses 36, 69, and 77, which have 3700 MW total installed capacity. For the hydrogen supply chain planning, we partition the system into three zones. Candidate hydrogen production, transportation, and storage infrastructures are also incorporated.

With our proposed joint planning model, the total annualized investment and operational cost reduces from  $166.46 \times 10^6$  \$ in the separate model to  $161.37 \times 10^6$  \$. In the investment decision from the joint planning model, we found two fewer lines are needed to be built. The annual utilization rate of renewable energy increases from 81.03% to 86.49%. These benefits from the joint planning model align with our previous analysis for the extended Garver's system.

2) *Sensitivity Analysis*: We notice that pipelines are not selected to construct for hydrogen transportation. Given the expectation of pipeline cost reduction with the deep development of hydrogen supply chain infrastructure, sensitivity analysis is interesting to conduct for pipeline investment cost. Fig. 12 shows the pipeline investment cost reduction percentage versus total system cost and pipeline investment by using our proposed co-planning model. As indicated, the total system cost is reduced as pipeline investment cost decreases. Meanwhile, more pipelines would be built when the cost is reduced by 25%, which results in the increase of pipeline investment

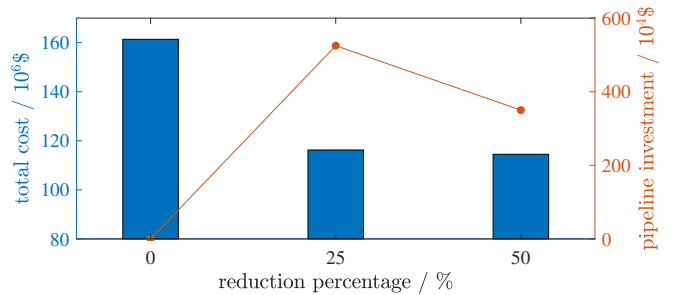


Fig. 12. Sensitivity analysis of pipeline investment cost.

in comparison to the original case (wherein pipelines are not selected). When the reduction percentage reaches 50%, the pipeline investment decreases, because the number of planned pipelines doesn't increase a lot while the cost of each pipeline is reduced. The sensitivity analysis indicates pipeline cost is important for total system cost reduction in the future.

## VI. CONCLUSION

This paper proposes a joint planning approach for electric power transmission and hydrogen transportation networks to achieve complementation from resources in power and hydrogen systems. This approach is further extended under a robust optimization framework to hedge against uncertainties. The numerical results show the proposed approach can benefit the two systems in overall cost reduction, renewable energy curtailment reduction, and transmission line utilization level increase. Our proposed linear continuous flexible truck routing model can quantify tank storage flexibility and transportation time delay. The hydrogen storage model can reflect the seasonal cycling requirement in representative week settings. Further research can focus on investigating coordination strategies for different operators of power and hydrogen systems, and incorporating alternating current power flow (ACPF) model in our proposed framework.

## REFERENCES

- [1] Wikipedia. (2020) Carbon neutrality. [Online]. Available: [https://en.wikipedia.org/wiki/Carbon\\_neutrality](https://en.wikipedia.org/wiki/Carbon_neutrality)
- [2] A. Chowdhury and D. O. Koval, "Deregulated transmission system reliability planning criteria based on historical equipment performance data," *IEEE Transactions on Industry Applications*, vol. 37, no. 1, pp. 204–211, 2001.
- [3] G. Latorre, R. D. Cruz, J. M. Areiza, and A. Villegas, "Classification of publications and models on transmission expansion planning," *IEEE Transactions on Power Systems*, vol. 18, no. 2, pp. 938–946, 2003.
- [4] B. Vatani, B. Chowdhury, and J. Lin, "The role of demand response as an alternative transmission expansion solution in a capacity market," *IEEE Transactions on Industry Applications*, vol. 54, no. 2, pp. 1039–1046, 2017.
- [5] Y.-K. Wu, C.-Y. Lee, C.-R. Chen, K.-W. Hsu, and H.-T. Tseng, "Optimization of the wind turbine layout and transmission system planning for a large-scale offshore windfarm by ai technology," *IEEE Transactions on Industry Applications*, vol. 50, no. 3, pp. 2071–2080, 2013.
- [6] J. Zhan, C. Chung, and A. Zare, "A fast solution method for stochastic transmission expansion planning," *IEEE Transactions on Power Systems*, vol. 32, no. 6, pp. 4684–4695, 2017.
- [7] C. Ruiz and A. J. Conejo, "Robust transmission expansion planning," *European Journal of Operational Research*, vol. 242, no. 2, pp. 390–401, 2015.

- [8] W. Xiao, Y. Cheng, W.-J. Lee, V. Chen, and S. Charoensri, "Hydrogen filling station design for fuel cell vehicles," *IEEE Transactions on Industry Applications*, vol. 47, no. 1, pp. 245–251, 2010.
- [9] B. Gim, K. J. Boo, and et al, "A transportation model approach for constructing the cost effective central hydrogen supply system in Korea," *International Journal of Hydrogen Energy*, vol. 37, no. 2, pp. 1162–1172, 2012.
- [10] J. André, S. Auray, J. Brac, D. De Wolf, G. Maisonnier, M.-M. Ould-Sidi, and A. Simonnet, "Design and dimensioning of hydrogen transmission pipeline networks," *European Journal of Operational Research*, vol. 229, no. 1, pp. 239–251, 2013.
- [11] S. Klyapovskiy, S. You, H. Cai, and H. W. Bindner, "Integrated planning of a large-scale heat pump in view of heat and power networks," *IEEE Transactions on Industry Applications*, vol. 55, no. 1, pp. 5–15, 2018.
- [12] Z. Li, C. Wang, B. Li, J. Wang, P. Zhao, W. Zhu, M. Yang, and Y. Ding, "Probability-interval-based optimal planning of integrated energy system with uncertain wind power," *IEEE Transactions on Industry Applications*, vol. 56, no. 1, pp. 4–13, 2019.
- [13] J. Li, J. Lin, and et al, "Optimal investment of electrolyzers and seasonal storages in hydrogen supply chains incorporated with renewable electric networks," *IEEE Transactions Sustainable Energy*, vol. 11, no. 3, pp. 1773–1784, 2020.
- [14] G. He, D. S. Mallapragada, A. Bose, C. F. Heuberger, and E. Gençer, "Hydrogen supply chain planning with flexible transmission and storage scheduling," *IEEE Transactions on Sustainable Energy*, vol. 12, no. 3, pp. 1730–1740, 2021.
- [15] B. Zeng and L. Zhao, "Solving two-stage robust optimization problems using a column-and-constraint generation method," *Operations Research Letters*, vol. 41, no. 5, pp. 457–461, 2013.
- [16] R. Jiang, J. Wang, and Y. Guan, "Robust unit commitment with wind power and pumped storage hydro," *IEEE Transactions on Power Systems*, vol. 27, no. 2, pp. 800–810, 2011.
- [17] Y. Wen, C. Guo, H. Pandžić, and D. S. Kirschen, "Enhanced security-constrained unit commitment with emerging utility-scale energy storage," *IEEE Transactions on Power Systems*, vol. 31, no. 1, pp. 652–662, 2015.
- [18] L. Bahiense, G. C. Oliveira, M. Pereira, and S. Granville, "A mixed integer disjunctive model for transmission network expansion," *IEEE Transactions on Power Systems*, vol. 16, no. 3, pp. 560–565, 2001.
- [19] R. Jiang, M. Zhang, G. Li, and Y. Guan, "Two-stage network constrained robust unit commitment problem," *European Journal of Operational Research*, vol. 234, no. 3, pp. 751–762, 2014.
- [20] S. Wang, G. Geng, and Q. Jiang, "Robust co-planning of energy storage and transmission line with mixed integer recourse," *IEEE Transactions on Power Systems*, vol. 34, no. 6, pp. 4728–4738, 2019.
- [21] IBM. ILOG CPLEX Homepage. Armonk, NY, USA. [Online]. Available: <http://www.ilog.com>
- [22] L. L. Garver, "Transmission network estimation using linear programming," *IEEE Transactions on Power Apparatus and Systems*, no. 7, pp. 1688–1697, 1970.
- [23] P. Fernández-Porras, M. Panteli, and J. Quirós-Tortós, "Intentional controlled islanding: when to island for power system blackout prevention," *IET Generation, Transmission & Distribution*, vol. 12, no. 14, pp. 3542–3549, 2018.
- [24] IIT. Data for IEEE 118-bus system. Chicago, IL, USA. [Online]. Available: [http://motor.ece.iit.edu/data/SCUC\\_118/SCUC\\_118.xls](http://motor.ece.iit.edu/data/SCUC_118/SCUC_118.xls)

**Siyuan Wang** received the B.S. and Ph.D. degrees in electrical engineering from Zhejiang University, Hangzhou, China, in 2013 and 2019, respectively. He is currently a Postdoctoral Fellow with the Department of Electrical and Computer Engineering, Missouri University of Science and Technology (formerly University of Missouri-Rolla), Rolla, MO, USA. His research interests include power system planning and operation, renewable energy integration, and the application of energy storage technology in power systems.

**Rui Bo** (Senior Member, IEEE) received the BSEE and MSEE degrees in electric power engineering from Southeast University (China) in 2000 and 2003, respectively, and received the Ph.D. degree in electrical engineering from the University of Tennessee, Knoxville (UTK) in 2009. He is currently an Assistant Professor of the Electrical and Computer Engineering Department with the Missouri University of Science and Technology (formerly University of Missouri-Rolla). He worked as a Principal Engineer and Project Manager at Midcontinent Independent System Operator (MISO) from 2009 to 2017. His research interests include computation, optimization and economics in power system operation and planning, high performance computing, electricity market simulation, evaluation and design.